Schulz, G. E., & Schirmer, R. H. (1979) *Principles of Protein Structure*, Springer-Verlag, New York.
Schweitz, H., Vincent, J.-P., Barhanin, J., Frelin, C., Linden, G., Hugues, M., & Lazdunski, M. (1981) *Biochemistry 20*, 5245-5252.
Scriabine, A., van Arman, C. G., Morgan, G., Morris, A. A., Bennett, C. D., & Bohidar, N. R. (1979) *J. Cardiovasc. Pharmacol. 1*, 571-583.
Shibata, S., Norton, T. R., Izumi, T., Matsuo, T., & Katsuki, S. (1976) *J. Pharmacol. Exp. Ther. 199*, 298-309.
Venkatachalam, C. M. (1968) *Biopolymers 6*, 1425-1436.
Wemmer, D., & Kallenbach, N. R. (1983) *Biochemistry 22*, 1901-1906.
Williamson, M. P., Havel, T. F., & Wüthrich, K. (1985) *J. Mol. Biol. 182*, 295-315.
Wunderer, G., & Eulitz, M. (1978) *Eur. J. Biochem. 89*, 11-17.
Wunderer, G., Fritz, H., Wachter, E., & Machleidt, W. (1976) *Eur. J. Biochem. 68*, 193-198.
Wüthrich, K. (1983) *Biopolymers 22*, 131-138.
Wüthrich, K., Billeter, M., & Braun, W. (1984) *J. Mol. Biol. 180*, 715-740.

Two-Dimensional ^{1}H NMR of Three Spin-Labeled Derivatives of Bovine Pancreatic Trypsin Inhibitor†

Phyllis Anne Kosen, Ruud M. Scheek, Hossein Naderi, Vladimir J. Basus, Sadasivam Manogaran, Paul G. Schmidt,‡ Norman J. Oppenheimer, and Irwin D. Kuntz*

Department of Pharmaceutical Chemistry, University of California, San Francisco, California 94143

Received October 21, 1985; Revised Manuscript Received December 19, 1985

ABSTRACT: Three nitroxide spin-labeled monoderivatives of bovine pancreatic trypsin inhibitor were prepared with the amino-specific reagent succinimidyl 1-oxy-2,2,5,5-tetramethyl-3-pyrroline-3-carboxylate. The monoderivatives were purified by ion-exchange and affinity chromatography. Thin-layer maps of tryptic peptides of the monoderivatives showed that the spin-label was incorporated at either the α-amino group, Lys-15, or Lys-26. Two-dimensional *J*-correlated ^{1}H NMR spectra of the monoderivatives were recorded. Spectra were also recorded after reduction by ascorbic acid of the nitroxide label to hydroxylamine. With the nitroxide label present, significant line-broadening effects on many of the cross peaks in the spectra were observed. The extent of line broadening for the $C_\alpha H$–NH cross peaks was qualitatively correlated with the distance between the labeled amino group and the average $C_\alpha H$–NH position in the crystal structure. The spin-label affects cross peaks of protons within ~15 Å. This study suggests that it is feasible to accumulate sufficient intramolecular distances in order to determine protein solution structures with the aid of distance geometry algorithms.

The advent of high-field two-dimensional NMR[1] spectroscopy has created a renewed interest in obtaining time-averaged solution conformations of macromolecules at a resolution comparable to that of X-ray crystallography. Wüthrich and his colleagues pioneered the combined use of the nuclear Overhauser effect, vicinal coupling constants, and hydrogen exchange rates obtained from two-dimensional spectra to identify regions of secondary structure in proteins (Wagner & Wüthrich, 1982b; Hosur et al., 1983; Pardi et al., 1983; Williamson et al., 1984). As a complementary approach, they have suggested using hydrogen–hydrogen through-space distances obtained from NOESY experiments in conjunction with distance geometry calculations (Havel et al., 1979, 1983; Havel & Wüthrich, 1985) to determine the three-dimensional structure of a protein (Braun et al., 1981, 1983; Wüthrich et al., 1982; Williamson et al., 1985). Others have made a similar suggestion with reference to nucleic acid structure (James et al., 1985). However, as only distances of less than 5 Å can be obtained from NOE studies, the number of distances measured is perhaps an order of magnitude smaller than needed for a medium-resolution protein structure (Havel et al., 1979; Havel & Wüthrich, 1985). Other techniques yielding nonredundant atom to atom distances must be developed to achieve a structure approaching 3-Å resolution.

Recently, reports by two groups have shown that distances between approximately 10 and 20 Å can be extracted from one-dimensional high-resolution NMR data, by incorporating a single nitroxide spin-label into a macromolecule. The distances were found with the distance dependence of the line broadening due to the dipolar relaxation of a given hydrogen by the paramagnetic electron of the spin-label (Solomon & Bloembergen, 1956). Schmidt and Kuntz (1984), repeating

†Supported by Grants GM-19267 (I.D.K.), RR-01695 (I.D.K.), and CA26272 (N.J.O.) from the National Institutes of Health. R.M.S. was supported by a fellowship from the Netherlands Organization for the Advancement of Pure Research (ZWO) and V.J.B. by a grant from the Academic Senate, University of California. The UCSF Magnetic Resonance Laboratory was partially funded by grants from the National Science Foundation (DMB 8406826) and the National Institutes of Health (RR-01668).

‡Present address: Vestar Research Inc., Pasadena, CA 91106.

[1] Abbreviations: NMR, nuclear magnetic resonance; NOESY, two-dimensional nuclear Overhauser enhancement spectroscopy; NOE, nuclear Overhauser enhancement; F_{ab}, N-terminal half of the heavy chain and the whole light chain of immunoglobulin G; COSY, two-dimensional *J*-correlated spectroscopy; BPTI, bovine pancreatic trypsin inhibitor; HPLC, high-performance liquid chromatography; TPCK, L-1-(tosylamido)-2-phenylethyl chloromethyl ketone; CM, carboxymethyl; FPLC, fast-performance liquid chromatography; Tris, tris(hydroxymethyl)-aminomethane; UV, ultraviolet.

0006-2960/86/0425-2356$01.50/0

an earlier experiment (Wien et al., 1972), incorporated a nitroxide spin-label at the single histidine of hen egg white lysozyme. They measured the line broadening on some 20 lysozyme hydrogen NMR resonances from the one-dimensional difference spectrum obtained by subtracting the spectrum of lysozyme with the nitroxide group present from that of the same sample after reduction of the nitroxide to the diamagnetic hydroxylamine. After the paramagnetic line broadening contributions were determined by a convolution difference technique, distances were calculated. The electron spin could be uniquely located in a groove on the protein's surface with the aid of distance geometry algorithms.

Along somewhat different lines, McConnell and co-workers are mapping the hapten combining site of an F_{ab} monoclonal antibody fragment by observing the line broadenings due to a spin-labeled dinitrophenol hapten (Anglister et al., 1984a,b, 1985; Frey et al., 1984). They have identified many of the amino acids within 17 Å of the hapten binding site by analyzing a variety of one-dimensional NMR difference spectra of selectively deuterated F_{ab} fragments in the presence/absence of spin-labeled and diamagnetic hapten. In favorable cases, specific distances have been extracted from the data.

The theory behind the aforementioned studies is not new nor is the qualitative observation of the line-broadening effect [e.g., Wien et al. (1972) and Dwek et al. (1975)]; rather improved NMR instrumentation allows the quantification of line-broadening effects because of better resolution and sensitivity. Thus, the means by which longer distances can be measured are available, but the results to date still fall short of a generalized protocol for obtaining the necessary number of distances used in distance geometry calculations. Even at 500 MHz, one-dimensional spectra show extensive overlap of hydrogen resonances for proteins the size of lysozyme or the F_{ab} fragment. This overlap problem limited the number of measurements that Schmidt and Kuntz made; selective deuteration was needed in the F_{ab} studies in part to simplify the difference spectra. As a possible way of circumventing this problem, we turned to two-dimensional NMR and decided to examine the line-broadening effects on the cross peaks in a COSY spectrum of a spin-labeled protein. Moonen et al. (1984) recently showed that line-broadening effects on the cross peaks of a protein's two-dimensional NMR spectrum due to the presence of a paramagnetic center can be observed. They obtained a NOESY difference spectrum of *Megasphaera elsdenii* flavodoxin from spectra with the protein's prosthetic group riboflavin 5′-monophosphate in its diamagnetic (hydroquinone) and paramagnetic (semiquinone) states.

For this work, we chose the protein bovine pancreatic trypsin inhibitor (BPTI), which has been extensively studied by two-dimensional NMR techniques (Wagner & Wüthrich, 1982a,b; Pardi et al., 1983; Stassinopoulou et al., 1984) and has also served as a primary example in both experimental and theoretical protein dynamics and protein folding studies [reviewed in McCammon & Karplus (1983) and Creighton (1985)].

As an additional point of interest, we have tested our ability to separate spin-labeled monoderivatives from a starting mixture of monoderivatives, diderivatives, and higher order derivatives when a spin-label is incorporated in a nonsite-specific manner. In the absence of chemical synthesis of the entire protein and because more than one spin-labeled monoderivative will be needed to accumulate a sufficient number of distances, a general method cannot rely on site-specific labels. It must rely on separation of monoderivatives from a mixture generated by nonspecific derivatization.

In this paper we present the high-resolution COSY "fingerprint" regions containing the $C_\alpha H$–NH proton cross peaks of three BPTI monoderivatives spin-labeled at amino groups by succinimidyl 1-oxy-2,2,5,5-tetramethyl-3-pyrroline-3-carboxylate.

Materials and Methods

Materials. Bovine pancreatic trypsin inhibitor (Trasylol) was obtained from Mobay Chemical Corp. Succinimidyl 1-oxy-2,2,5,5-tetramethyl-3-pyrroline-3-carboxylate, a product of Molecular Probes Inc., was recrystallized from HPLC-grade methanol, cor mp 179–181 °C. Organic solvents were obtained through Fisher Scientific or Mallinckrodt Inc. Fluorescamine came from Pierce Chemical Co., ninhydrin from Nutritional Biochemicals Corp., and cadmium acetate from Alfa Products. Sigma Chemical Co. was the source of the all other reagents except as noted in the text. TPCK-treated trypsin was assayed by the method of Chase and Shaw (1967) using the active site titrant *p*-nitrophenyl *p*′-guanidinobenzoate hydrochloride. Chymotrypsin–Sepharose was prepared by the method of March et al. (1974). Two grams of chymotrypsin (type II, Sigma) was coupled by the CNBr method to 100 mL of Sepharose 4B-200. Approximately 1.8 mg of BPTI bound per milliliter of resin.

Preparation of Spin-Labeled Monoderivatives of BPTI. Approximately 30 μmol of BPTI in 7.5 mL of 50 mM sodium phosphate, pH 7.2, and an equimole amount of succinimidyl 1-oxy-2,2,5,5-tetramethyl-3-pyrroline-3-carboxylate in a small volume of HPLC-grade acetonitrile were mixed in the dark, overnight at room temperature (Rousselet et al., 1984). The buffer was changed to 20 mM imidazole, pH 6.2, by elution on a 2.5 × 20 cm column of Sephadex G-25. This solution was applied to a 1.5 × 25 cm CM-cellulose column (CM-52, Whatman Ltd.) equilibrated with 20 mM imidazole, pH 6.2, at room temperature. A linear gradient of 0.0–0.3 M NaCl, total volume of 700 mL, was used to elute the spin-labeled BPTI derivatives.

Fraction 2 of the CM-cellulose profile shown in Figure 1 was concentrated by lyophilization, desalted in 0.5% ammonium bicarbonate, lyophilized, and dissolved at a concentration of approximately 5 mg/mL in 50 mM ammonium acetate, pH 4.0. Two monoderivatives were then separated by the Pharmacia FPLC chromatography system with two Mono-S HR 5/5 columns (a strong cation exchanger) connected in series and an isocratic gradient, 0.83 M in ammonium acetate, pH 4.0.

The CM-cellulose fractions containing the monoderivative spin-labeled at Lys-15 and additional derivatives (fraction 1 of Figure 1) were pooled and concentrated by lyophilization, and the salts were changed to 0.1 M Tris-HCl, pH 8.0 (at 4 °C), 0.5 M NaCl, and 10 mM $CaCl_2$ by elution over Sephadex G-25. This protein mixture was applied to a chymotrypsin–Sepharose column (containing enough chymotrypsin to bind at least a mole equivalent of the applied BPTI derivatives) at 4 °C. The column was developed by first washing with slightly more than 1 column volume of the Tris–NaCl–$CaCl_2$ buffer and then with 0.01 M HCl, 0.5 M NaCl, and 10 mM $CaCl_2$. The salts of pooled protein peaks were exchanged over Sephadex G-25 with 0.5% ammonium acetate, and the ammonium acetate was removed by lyophilization. All purified derivatives were stored at −20 °C in lyophilized form.

Identification of the Spin-Labeled Monoderivative Sites by Peptide Mapping and Amino Acid Analysis. Denatured protein was prepared for trypsin treatment by one of two methods: BPTI or the monoderivatives were dissolved in performic acid (Hirs, 1967) at a concentration of 1 mg/mL,

at −4 to −5 °C, incubated for 1.5 h, and lyophilized. Alternatively, protein was dissolved at a concentration of 3 mg/mL in a degassed solution containing 0.2 M Tris-HCl, pH 8.6, 6 M guanidine hydrochloride, 10 mM ethylenediaminetetraacetic acid, and a 20 mol excess (over protein) of dithiothreitol. After 0.5 h, 0.37 mL of 0.5 M iodoacetic acid, 0.5 M KOH, and 0.2 M Tris-HCl, pH 8.6, was added per milliliter of protein solution, and alkylation proceeded for 15 minutes. The protein was desalted over Sephadex G-25 in 0.1 M HCl and lyophilized.

Denatured protein, with the disulfides either oxidized to cysteic acid or reduced and carboxymethylated, was added to 0.1 M ammonium bicarbonate, pH 8.2, at an approximate concentration of 2 mg/mL. The protein was digested with TPCK-treated trypsin for 2 h at 37 °C at a substrate to active enzyme ratio of 100:1 (w/w). A further 1% by weight addition of trypsin was made and incubation continued for an additional 2 h. The solution was centrifuged, and to the supernatant a final 1% addition of trypsin was made. After incubation overnight, the digest was lyophilized, and then dissolved at a nominal concentration of 15 mg/mL in 20% pyridine.

The peptide digest was analyzed by two-dimensional peptide mapping on thin-layer cellulose sheets (Kodak Chromagram) with ascending chromatography in butanol–acetic acid–pyridine–H_2O (15:3:10:12 v/v/v/v) in the first dimension for 4–5 h, followed by electrophoresis at 400 V for 1.25 h in pyridine–acetic acid–H_2O–acetone (50:2.5:347.5:100 v/v/v/v) in the second dimension. The peptides were located by ninhydrin/cadmium acetate (Heilmann et al., 1957) or by dipping the plates in 3% pyridine/acetone, followed by dipping in 0.001% fluorescamine/acetone and visualizing under UV light. Peptides were also examined for their arginine content with phenanthrenequinone (Yamada & Itano, 1966) and for their tyrosine content with nitrosonaphthol (Easley, 1965).

In preparation for amino acid analysis, peptides, located by fluorescamine treatment, were recovered by scraping them off the cellulose gel. The peptides were eluted into 50% pyridine, filtered through Whatman GF/B fiber paper, and lyophilized in a hydrolysis tube. One milliliter of 6 M HCl with 0.0067% β-mercaptoethanol was added to each peptide sample, degassed under reduced pressure, and hydrolyzed at 110 °C for 20 h. A Beckman 119 CL automated amino acid analyzer was used for the analyses.

Concentration Measurements. The concentrations of spin-labeled monoderivative solutions were routinely determined with an extinction coefficient of 5900 L/(cm·mol) at 280 nm. This extinction coefficient is simply the sum of those of BPTI (Kassell, 1970) and of 1-oxy-2,2,5,5-tetramethyl-3-pyrroline-3-carboxylic acid (Molecular Probes Inc.). The validity of the use of this extinction coefficient was tested as follows. Concentrations of monoderivatives were determined by the method of Lowry et al. (1951) with BPTI as the protein standard and compared to the concentrations of the same solutions determined with 5900 L/(cm·mol). Within the uncertainties (<±5%) of the Lowry method, the two concentration measurements were in agreement.

NMR Spectroscopy. Two-dimensional *J*-correlated (COSY) spectra were recorded on a 500-MHz GE-Nicolet spectrometer, interfaced to a Nicolet 1280 computer. The $(90°–t_1–90°–t_2)_n$ pulse sequence described by Aue et al. (1976) was used. The water signal was suppressed by presaturation during the 2–3-s relaxation delay (Kumar et al., 1980).

For the spectra of the monoderivatives, 512 free induction decays, each of 1024 complex data points were recorded with a ±3512-Hz spectral width, with the carrier positioned at the

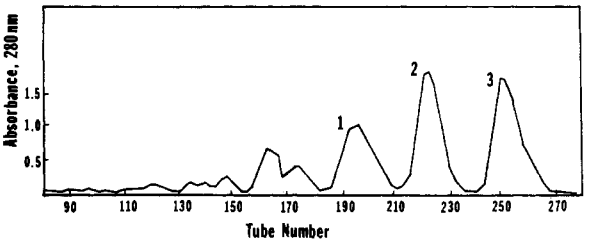

FIGURE 1: CM-cellulose chromatography of the reaction mixture of BPTI and succinimidyl 1-oxy-2,2,5,5-tetramethyl-3-pyrroline-3-carboxylate. Each aliquot contained approximately 2 mL. Fraction 3 is unmodified BPTI. Fractions 1 and 2 contained mixtures of monoderivatives and were further purified as described in the text.

H_2O resonance frequency. Eight or sixteen scans were accumulated for each t_1 value. The data were weighed with an unshifted sine-bell function in both domains before zero filling and Fourier transformation. The resulting spectra (1024 × 2048 data points) are presented in the absolute-value mode. The base lines of the spectra were fitted to a sixth-order polynomial and corrected in ω_1 (Pearson, 1977). By this procedure, "t_1 ridges" (Denk et al., 1985) are suppressed, and regions containing only noise will have zero integrated intensity. Cross-peak intensities were measured by defining squares around individual peaks and summing up the spectral intensities within these squares.

The NMR samples contained 2 mM protein in 90% H_2O/10% D_2O (0.4–0.5 mL total volume) at pH 2 and 68 °C. Reduction of the spin-label was achieved by addition of approximately 100% excess in reducing equivalents of ascorbic acid in 5 μL at pH 2.

For BPTI itself, we recorded a double-quantum-filtered COSY spectrum of 1024 free induction decays (using time-proportional phase incrementation), each of 1024 complex data points. Sixteen scans were accumulated for each t_1 value. The protein concentration was 6 mM under otherwise identical conditions (68 °C, pH 2.0).

Results and Discussion

Purification of Spin-Labeled Monoderivatives of BPTI. Reaction of equimolar succinimidyl 1-oxy-2,2,5,5-tetramethyl-3-pyrroline-3-carboxylate and BPTI resulted in a complex mixture of spin-labeled protein. This was expected. Although the reaction is specific for amino groups, there are five potentially reactive sites in BPTI—at the α-amino group of Arg-1 and at each of the ϵ-amino groups of Lys-15, -26, -41, and -46. No single purification technique proved adequate for complete separation of the monoderivatives, and a more involved procedure was developed. For simplicity, the purification is outlined in terms of the subsequently identified spin-labeled monoderivatives. Details of their characterization will be given in the next section.

Partial isolation of the monoderivatives was obtained by CM-cellulose chromatography of the whole reaction mixture, Figure 1. Unreacted protein and many of the multiply labeled derivatives were cleanly separated from the monoderivatives, which migrated in fractions 1 and 2 of the elution profile.

Fraction 2 was resolved into two monoderivatives on the FPLC Mono-S chromatography system described under Materials and Methods (chromatography not shown). The α-amino spin-labeled derivative eluted first, followed by the Lys-26 derivative. For maximum resolution, it was necessary to connect two Mono-S columns in series and to perform two to three rounds of chromatography. Final yields were approximately 12% of starting protein for each of these derivatives.

Table I: Amino Acid Composition of Peptide Fragments of BPTI after Tryptic Digest[a]

	peptide											
amino acid	1–15	16–17	18–20	21–23[b]	24–26	27–33	34–39[b]	40–41	40–42[c]	43–46	47–53	54–58
cysteic acid	2.5 (2)					1.0 (1)	NQ (1)[d]				1.0 (1)	1.2 (1)
aspartic acid	1.2 (1)				0.87 (1)		0.42 (0)			1.8 (2)	2.0 (1)[e]	
threonine	0.62 (1)					1.1 (1)						0.49 (1)[f]
serine	0.18 (0)										0.29 (1)[f]	0.12 (0)
glutamic acid	1.1 (1)					1.0 (1)				0.33 (0)	0.95 (1)	
proline	4.5 (4)					0.14 (0)						
glycine	1.4 (1)	0.16 (0)	0.58 (0)	0.24 (0)	0.14 (0)	1.1 (1)	2.4 (2)	0.22 (0)	1.3 (0)		0.24 (0)	2.1 (2)
alanine		1.0 (1)			1.0 (1)	0.92 (1)		1.0 (1)	1.0 (1)		1.0 (1)	1.0 (1)
valine							1.0 (1)					
isoleucine			1.7 (2)									
leucine	1.0 (1)					1.0 (1)						
tyrosine	0.84 (1)			1.5 (2)			0.85 (1)					
phenylalanine	0.97 (1)			1.0 (1)		1.0 (1)				1.0 (1)		
lysine	0.86 (1)				0.80 (1)			0.81 (1)	1.0 (1)	0.87 (1)		
arginine	0.76 (1)	0.94 (1)	1.0 (1)				1.0 (1)		0.84 (1)		0.89 (1)	

[a] Peptides are given by their amino acid sequence. Numbers in parentheses give the expected amino acid contribution. The greatest level of contaminating amino acid is given. [b] Peptides 21–23 and 34–39 were identified from TLC maps of the Lys-15 spin-label derivative. As explained in the text, they were overlooked originally, and to expedite their identification, new performic acid oxidized BPTI digests were not prepared. [c] This peptide was recovered in low yields. The amount of glycine present was similar to that of background levels for many of the other peptides for which glycine was the greatest contaminant. [d] NQ not quantitated; CM-Cys was present. [e] Also contains methionine sulfone. This peptide has one methionine. [f] The N-terminal amino acid. Partial destruction by fluorescamine and by acid hydrolysis could account for the low recovery.

The monoderivative spin-labeled at Lys-15 was found in fraction 1 of the CM-cellulose elution profile. To separate the Lys-15 derivative from other spin-labeled species, we took advantage of the fact that BPTI inhibits serine proteases by binding with its Lys-15 side chain oriented in the enzyme binding pocket (Vincent & Lazdunski, 1973). As shown in Figure 2, a portion of the CM-cellulose fraction 1 did not bind when applied to chymotrypsin–Sepharose. This was as expected for a Lys-15 derivative. This derivative was homogeneous by all criteria (see below) and accounted for 5–7% of the starting material.

The protein that bound to chymotrypsin was eluted at low pH, where the chymotrypsin–BPTI complex is not stable. This mixture could be further fractionated by Mono-S chromatography with an isocratic 0.79 M ammonium acetate, pH 4.0, gradient (chromatography not shown). A putative monoderivative eluted first, followed by a derivative or derivatives with more than one bound nitroxide label. Although the monoderivative appeared homogeneous by three of our criteria, its peptide map was ambiguous—all of the possible tryptic peptides of unmodified BPTI were present (see below). As this monoderivative population accounted for no more than 5% of the starting material, no further attempts were made at separation.

Characterization of the Spin-Labeled Monoderivatives of BPTI. Three physical techniques were used to monitor the purification and homogeneity of the spin-labeled monoderivatives. Figure 3 shows the electrophoretic patterns of the monoderivatives on nondenaturing polyacrylamide gels at pH 3.8. Even at protein loads 3 times greater than those shown in the figure, no more than a single band was seen for each monoderivative. All of the isolated derivatives migrated as single symmetrical peaks when chromatographed on Mono-S resin with either the isocratic gradients mentioned previously or linear gradients of ammonium acetate at either pH 4.0 or 6.5. Finally, the UV spectrum of each derivative exhibited a maximum absorbance at 277.5 nm and a minimum absorbance at 256.8 nm. The ratio of the maximum to minimum absorbances was consistently 1.33 ± 0.03 for the purified monoderivatives.

As proof of homogeneity and to identify the spin-labeled residues, peptide maps of tryptic fragments of BPTI and the four separated monoderivative populations were examined.

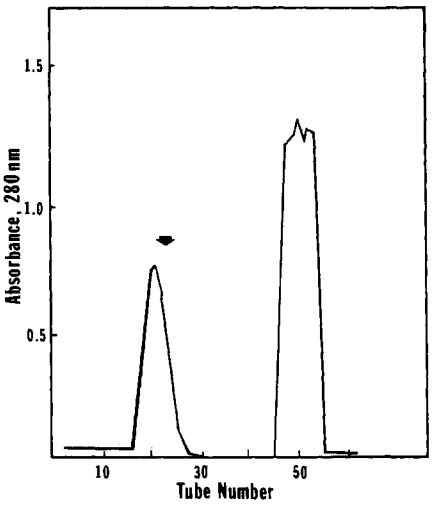

FIGURE 2: Chymotrypsin–Sepharose affinity chromatography of fraction 1 of the CM-cellulose chromatography. The arrow indicates the start of the acidic elution; other details are given under Materials and Methods.

Figure 4 diagrams the maps of BPTI and the three monoderivatives that proved to be homogeneous. Originally, the proteins were prepared for digestion by performic acid oxidation of the disulfides. Two complications were encountered when these maps were analyzed.

Given the amino acid sequence of BPTI, four anionic and six cationic peptides (plus free arginine) were expected after trypsin treatment. These were found as can be seen in the BPTI map. However, amino acid analysis (Table I) showed that peptides 24–26 and 27–33 arose not only from a trypsin-specific cleavage (at Lys-26) but also from chymotrypsin-like cuts, which were highly specific and complete at Tyr-23 and Phe-33. Because the amino groups that potentially could be spin-labeled and their surrounding peptide sequences were identified among the cationic and anionic peptides, no purification of the trypsin preparation was attempted. The two missing peptides, 21–23 and 34–39, were identified among the five neutral peptides in maps of totally carboxymethylated derivatives. Maps were first stained with either phenanthrenequinone, which is specific for arginine (Yamada & Itano, 1966), or with nitrosonaphthol, which is specific for

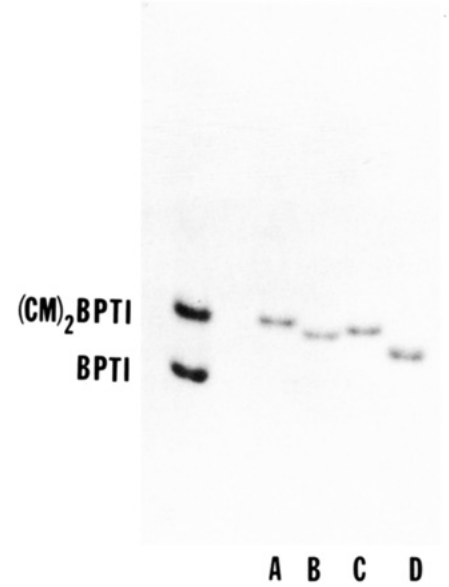

FIGURE 3: Electrophoretic profile of the spin-labeled BPTI monoderivatives. The low-pH discontinuous gel system of Reisfeld et al. (1962) was used in modified form. The separating gel was 12% in acrylamide (Ultragrade, LKB Instruments Inc.) and 1.25% in *N*,*N*′-methylenebis(acrylamide) at a pH of 4.3. The stacking gel was 2.5% in acrylamide and 0.6% in bis(acrylamide), pH 6.7. The electrophoresis buffer was 8 g/L in β-alanine and adjusted to pH 4.5 with acetic acid. Electrophoresis was at 200 V and 4 °C. The gel was stained with 0.05% Coomassie brilliant blue R-250 (Bio-Rad Laboratories), 10% trichloroacetic acid, and 10% sulfosalicylic acid and destained in 5% methanol–7.5% acetic acid. Each sample contained 5 μg of protein. Lane A is the Lys-26 monoderivative. Lane B is the α-amino monoderivative. Lane C is the Lys-15 monoderivative. Lane D is the fraction that bound chymotrypsin–Sepharose and was further purified on Mono-S resin using the 0.79 M ammonium acetate isocratic gradient. Although it appeared homogeneous by the criterion of gel electrophoresis, it may consist of two monoderivatives as discussed in the text. For comparison, the left-hand lane shows the migration of native BPTI and BPTI reduced and carboxymethylated at the disulfide formed by cysteine-14 and -38, $(CM)_2$BPTI.

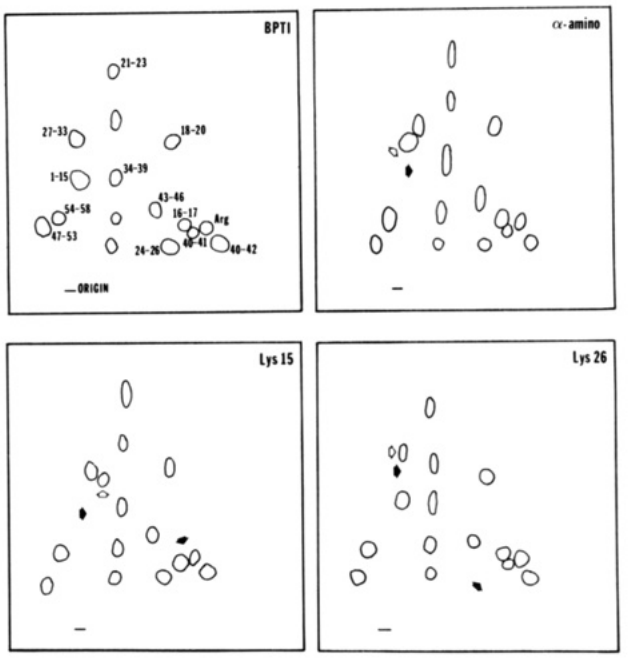

FIGURE 4: Diagrams of the two-dimensional thin-layer cellulose tryptic peptide maps of BPTI and the three purified monoderivatives. Chromatography was in the vertical direction and electrophoresis in the horizontal direction. The tryptic peptide maps of BPTI after performic acid oxidation and after reduction with dithiothreitol and carboxymethylation were identical. The sequences of the peptides, deduced from amino acid analysis, are indicated in the map of BPTI. The remaining three neutral peptides were not identified and are presumably redundant portions of the protein. The position labeled Arg is assumed to be free arginine. It migrated upon electrophoresis at the same rate as arginine and it was stained with ninhydrin but not with fluorescamine. Arginine would arise from the partial digestion of the Ala_{40}-Lys_{41}-Arg_{42} peptide. The other maps are for the derivatives after reduction and carboxymethylation. These maps are identical with those obtained after performic acid oxidation of the derivatives' disulfides, except that in the latter cases no new peptides could be found. The open arrows indicate the positions of the new peptides generated by the presence of the spin-label. The closed arrows indicate the positions of the peptides that are lost.

tyrosines (Easley, 1965). Only one of the five neutral peptides contained both arginine and tyrosine, and a second peptide stained only for tyrosine. The identities of these two peptides were confirmed by amino acid analysis.

To identify the positions of the spin-label, monoderivatives were prepared for trypsin treatment by reduction and carboxymethylation of the disulfides. In Figure 4, the open arrows indicate the positions of the new peptides that arose due to the presence of the spin-label and the solid arrows the positions of the original peptides present in the absence of the spin-label. The amino acid composition of the new peptides was determined (Table II) and clearly reveals that monoderivatives spin-labeled at the α-amino terminus and at the ε-amino groups of Lys-15 and Lys-26 had been purified. The map of the fourth monoderivative(s) was ambiguous and may be a mixture of Lys-41 and Lys-46 derivatives. The same peptides were absent in each of the performic acid oxidized monoderivative maps, but no new peptides were present. Thus, reduction and carboxymethylation were needed to confirm the identities of the monoderivatives. We do not understand why no new peptides were seen in the maps of performic acid oxidized derivatives.

NMR Spectroscopy. For BPTI itself (Figure 5) and for each of the purified monoderivatives (Figure 6), we obtained COSY spectra in H_2O. The protein concentrations of the monoderivatives were held to 2 mM, and the pH was adjusted to 2.0 with HCl to minimize effects of dimerization. Spectra

Table II: Amino Acid Composition of Peptides Generated by the Presence of Spin-Label on BPTI[a]

amino acid	α-amino[b,c]	Lys-15	Lys-26
aspartic acid	1.1 (1)	0.90 (1)	0.79 (1)
threonine	1.3 (1)	1.0 (1)	1.0 (1)
serine	0.44 (0)		0.41 (0)
glutamic acid	2.1 (1)	1.0 (1)	1.1 (1)
proline	3.0 (4)	3.4 (4)	
glycine	2.8 (1)	1.1 (1)	2.4 (1)
alanine	1.2 (0)	0.98 (1)	1.9 (2)
isoleucine		0.04 (0)	
leucine	1.6 (1)	1.0 (1)	1.0 (1)
tyrosine	0.72 (1)	0.74 (1)	
phenylalanine	1.0 (1)	1.0 (1)	0.87 (1)
lysine	1.1 (1)	0.96 (1)	0.92 (1)
arginine	0.77 (1)	1.5 (2)	

[a] Numbers in parentheses give the expected amino acid composition. The greatest level of contaminating amino acid is given. In all cases, CM-Cys was present but not quantitated. [b] Probably partially contaminated by peptide 27–33. All amino acids found in larger than expected amounts are also found in 27–33. [c] Heading indicates the spin-labeled monoderivative from which the peptide was derived.

were recorded at 68 °C. Two sets of spectra were obtained for the spin-labeled derivatives. The first used the purified paramagnetic sample; the second followed in situ reduction with 2-fold excess ascorbic acid.

The spectral region of most interest for this paper is the "fingerprint" region in which all the residues except proline

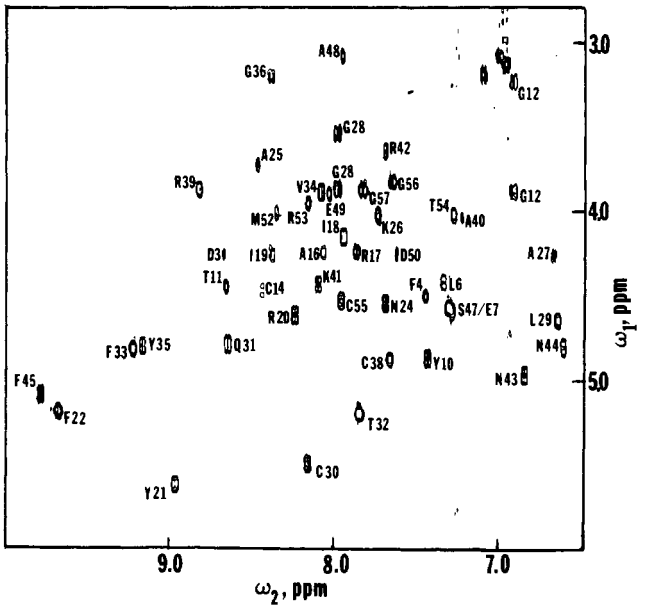

FIGURE 5: Fingerprint region (ω_2 = 10.6–6.6 ppm; ω_1 = 6.0–2.8 ppm) of the double-quantum-filtered COSY of unmodified BPTI, presented in the absolute-value mode for comparison with Figure 6. Cross-peak assignments are given with the one-letter code for the amino acids. The cross peaks of Cys-51 and Tyr-23 are outside the boundaries of this figure. Cross peaks of Cys-5, Lys-15, and Lys-46 are lost through interference with the H_2O resonance. The cross peaks of Ala-58 is also not seen at pH 2.0.

Table III: Trypsin Inhibitor Chemical Shifts (ppm), 68 °C, pH 2.0

Asp-3	4.30	8.70[a]	Gln-31	4.81	8.67
Phe-4	4.53	7.48[b]	Thr-32	5.24	7.88
Cys-5	4.27	7.26[a]	Phe-33	4.84	9.24
Leu-6	4.47	7.38[a,b]	Val-34	3.91	8.12
Glu-7	4.61	7.32[a]	Tyr-35	4.82	9.19[b]
Tyr-10	4.90	7.48[a,b]	Gly-36	3.23	8.42
Thr-11	4.48	8.70[b]	Cys-38	4.90	7.70
Gly-12	3.26, 3.88	6.96[b]	Arg-39	3.90	8.86[b]
Cys-14	4.50	8.47[b]	Ala-40	4.07	7.26[b]
Lys-15	4.40	7.77[b]	Lys-41	4.46	8.13[b]
Ala-16	4.27	8.10	Arg-42	3.66	7.72[a,b]
Arg-17	4.28	7.88[b]	Asn-43	5.00	6.89[a,b]
Ile-18	4.18	7.99	Asn-44	4.84	6.64
Ile-19	4.28	8.42[b]	Phe-45	5.12	9.81
Arg-20	4.65	8.26	Ser-47	4.58	7.34[a,b]
Tyr-21	5.66	9.00[b]	Ala-48	3.10	7.98
Phe-22	5.22	9.70	Glu-49	3.92	8.06[a,b]
Tyr-23	4.26	10.34[a,b]	Asp-50	4.28	7.66
Asn-24	4.58	7.73	Cys-51	1.76	6.94
Ala-25	3.76	8.50[b]	Met-52	4.04	8.39[a]
Lys-26	4.06	7.77	Arg-53	3.98	8.20
Ala-27	4.29	6.70	Thr-54	4.04	7.30
Gly-28	3.56, 3.87	8.00	Cys-55	4.58	8.00[b]
Leu-29	4.67	6.67	Gly-56	3.86	7.69[b]
Cys-30	5.53	8.20	Gly-57	3.92	7.88[b]

[a] Shifts of more than 0.10 ppm compared to the spectrum of BPTI at pH 4.6, 68 °C (Wagner & Wüthrich, 1982a). No chemical shift deviations of more than 0.10 ppm were seen for the C_α region. [b] Shifts of more than 0.10 ppm compared to the spectrum at pH 3.5, 50 °C (Pardi et al., 1983). No chemical shift deviations of more than 0.10 ppm were seen for the C_α region.

may show cross peaks arising from the J coupling between the C_α and NH protons. These spectra are shown in Figures 5 and 6. From the studies of Wüthrich and co-workers, we expected to find cross peaks for all residues except for the four prolines (2, 8, 9, and 13) and for Arg-1 and Gly-37, both of which have as yet escaped detection. Before we could analyze the results, proper assignment of the cross peaks was essential. The task of assignment for the BPTI NMR spectrum has been vigorously pursued in Wüthrich's laboratory. They have published the chemical shifts of virtually all the proton resonances under similar (i.e., 68 °C, pH 4.6) but not identical conditions. The bulk of our assignments could be taken directly from Wagner and Wüthrich (1982a). To identify cross peaks with altered positions due to the somewhat different conditions used in these experiments, we obtained a NOESY spectrum (not shown) to provide the relevant connectivities. The chemical shifts for the C_α and NH protons are given in Table III. The C_α proton of Lys-26 resonates at the H_2O frequency and is lost from the spectrum. Nor were we able to identify the cross peaks of Cys-5 and Lys-15, whose C_α protons are also close to the H_2O frequency at this pH. Further, no cross peak was found for the C-terminal alanine.

Chemical shifts that deviate by more than 0.10 ppm from those recorded by Wagner and Wüthrich (1982a) are noted in Table III. The deviations are readily understood in terms of the titration behavior of the carboxylic acids (Asp-3, Asp-50, Glu-7, Glu-49), the carboxyl terminal (Ala-58), and secondary effects of these groups on other residues. Additional chemical shift deviations are seen when changes in both pH and temperature occur (Pardi et al., 1983).

Turning our attention to the spin-labeled derivatives, we note that the chemical shifts are generally very similar to those of unmodified BPTI. The largest single deviation is 0.05 ppm. There are no significant differences of chemical shift on reduction of the spin-labels to the corresponding hydroxylamines. Thus, the derivatives are folded into structures very much like that of BPTI itself, and there are no significant structural perturbations either from the introduction of the label or from changes in the oxidation state.

We do call attention to a number of minor additional peaks that are noticeable in some of the COSY spectra. Such peaks have been seen by others in the spectrum of BPTI (Wagner & Wüthrich, 1982a; Stassinopoulou et al., 1984; P. Kim, personal communication). Whether these peaks arise from slowly interconverting conformational isomers or from actual covalent modifications (or both) is not clear at this time.

We return to our major theme, which is a qualitative assessment of the information we can obtain from the COSY spectra of the labeled derivatives. Quantitative analysis of the distance information is deferred until a later paper. The dominant effect of the introduction of an isotropic paramagnetic center into the protein is to broaden the proton resonances. The phenomenon is proportional to the inverse sixth power of the distance from the paramagnetic spin to the observed proton. It is also influenced by the overall tumbling of the protein and by local motions that affect the relative positions of the electron and proton spins (Solomon & Bloembergen, 1956). The result of line broadening is an intensity loss of cross peaks in COSY spectra caused by their antiphase character. As the antiphase components of a multiplet broaden, there will be more overlap resulting in mutual cancellation. Measurements of either peak height or integrated intensity are thus quite sensitive to broadening when W/J approximates 1 (Weiss et al., 1984), where W is the line width and J is the coupling constant.

As noted above, the complete analysis of the intensity changes is quite complicated. However, the selective effects of the labeling can be readily demonstrated simply by plotting the ratio of the paramagnetic and diamagnetic integrated intensities against the sequence number of the residue, as shown in Figure 7. This ratio should be 1 for resonances far from the label and approach zero for resonances whose protons are quite close to the label. Such behavior was observed (Figure 7) with a standard deviation of ~15%. Inspection

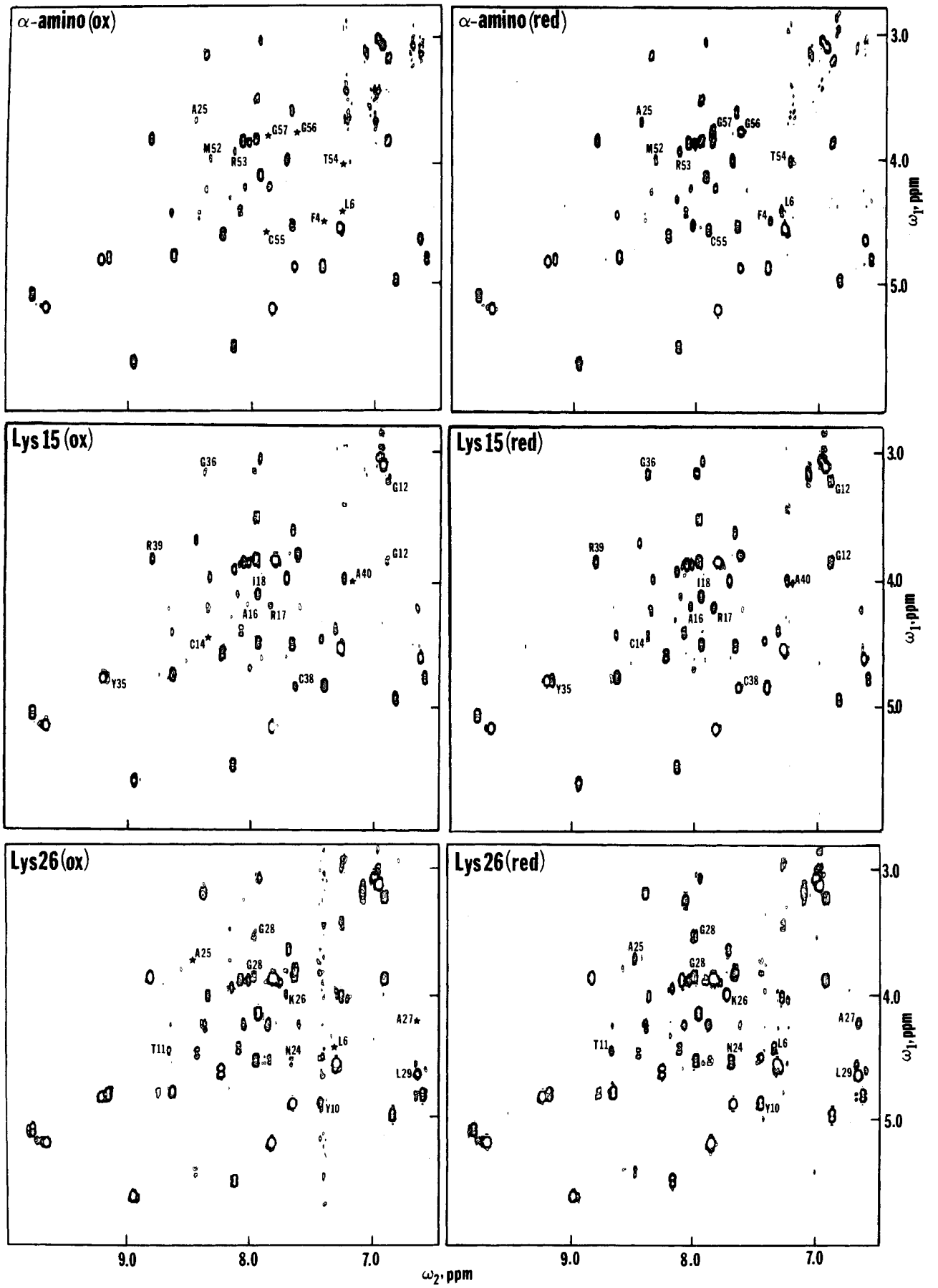

FIGURE 6: Fingerprint region (ω_2 = 10.6–6.6 ppm and ω_1 = 6.0–2.8 ppm) of the three spin-labeled monoderivatives' COSY spectra. For each derivative, the right-hand panel shows the spectrum after reduction of the label to the diamagnetic hydroxylamine and the left-hand panel that when the paramagnetic nitroxide was present. Cross-peak assignments are given with the one-letter code for amino acids. Stars mark the positions in the left-hand panels where cross peaks were below the minimum contour because of the paramagnetic line-broadening effect of the spin-label. Experimental conditions are given in the text.

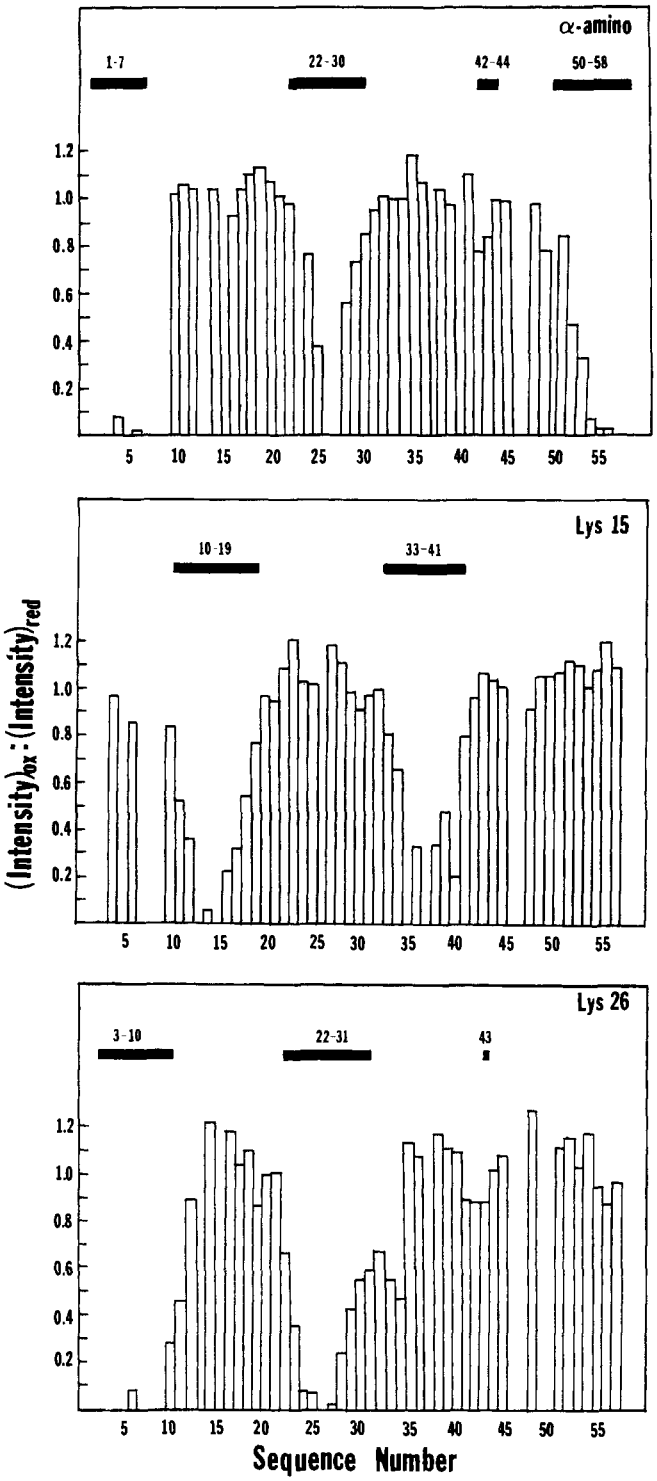

FIGURE 7: Ratio of the integrated cross-peak intensities measured in the spectra of the paramagnetic (oxidized) BPTI derivatives (left-hand panels of Figure 6) to those measured in the spectra of the diamagnetic (reduced) derivatives (right-hand panels of Figure 6) are plotted vs. the sequence position to which the cross peak corresponds. Gaps in the plot occur at positions where no cross peaks were found, where cross peaks overlapped, and in the single case of the cross peak of Gly-57 of the oxidized α-amino derivative where no intensity was measurable. The bars indicate residues with average $C_\alpha H$–NH distances to the amino group of the derivatized amino acid of less than 15 Å as calculated from the crystal coordinates of BPTI.

of the distances of the amide group of each residue from the amino terminus and the amino groups of Lys-15 and Lys-26 in the crystal structure (Deisenhofer & Steigemann, 1975) suggests that the present experiment readily detects protons within ~15 Å of the spin-labels. Approximately one-third of the residues are measurably affected in each derivative. Thus, paramagnetic line-broadening effects for some 20 amide protons and α-carbon protons and a larger number of side-chain protons can be measured for each spin-labeled derivative.

The primary goal of the work described in this paper was to prepare and characterize spin-labeled monoderivatives of BPTI. It is clear that the tasks of synthesis and purification of specifically labeled material from a protein of low molecular weight are feasible even if only nonspecific reagents are available. The utility of the spin-labeled derivatives for quantitative distance measurements will be addressed in a second paper. We are encouraged by the apparent sensitivity of the two-dimensional NMR experiments for measuring internal distances.

ACKNOWLEDGMENTS

We thank G. Crombie of Boston University School of Medicine for the amino acid analyses and R. Arnold, J. Shohet, and P. Babbitt for preliminary experiments.

Registry No. BPTI, 12407-79-3; BPTI (α-amino spin-labeled derivative), 101054-34-6; BPTI (Lys-15 spin-labeled derivative), 101054-35-7; BPTI (Lys-26 spin-labeled derivative), 101054-36-8; succinimidyl 1-oxy-2,2,5,5-tetramethyl-3-pyrroline-3-carboxylate, 100994-49-8.

REFERENCES

Anglister, J., Frey, T., & McConnell, H. M. (1984a) *Biochemistry 23*, 1138.

Anglister, J., Frey, T., & McConnell, H. M. (1984b) *Biochemistry 23*, 5372.

Anglister, J., Frey, T., & McConnell, H. M. (1985) *Nature (London) 315*, 65.

Aue, W. P., Bartholdi, E., & Ernst, R. R. (1976) *J. Chem. Phys. 64*, 2229.

Braun, W., Bösch, C., Brown, L. R., Gō, N., & Wüthrich, K. (1981) *Biochim. Biophys. Acta 667*, 377.

Braun, W., Wider, G., Lee, K. H., & Wüthrich, K. (1983) *J. Mol. Biol. 169*, 921.

Chase, T., Jr., & Shaw, E. (1967) *Biochem. Biophys. Res. Commun. 29*, 508.

Creighton, T. E. (1985) *J. Phys. Chem. 89*, 2452.

Deisenhofer, J., & Steigemann, W. (1975) *Acta Crystallogr. Sect. B: Struct. Crystallogr. Cryst. Chem. B31*, 238.

Denk, W., Wagner, G., Rance, M., & Wüthrich, K. (1985) *J. Magn. Reson. 62*, 350.

Dwek, R. A., Knott, J. C. A., March, D., McLaughlin, A. C., Press, E. M., Price, N. C., & White, A. I. (1975) *Eur. J. Biochem. 53*, 25.

Easley, C. W. (1965) *Biochim. Biophys. Acta 107*, 386.

Frey, T., Anglister, J., & McConnell, H. M. (1984) *Biochemistry 23*, 6470.

Havel, T. F., & Wüthrich, K. (1985) *J. Mol. Biol. 182*, 281.

Havel, T. F., Crippen, G. M., & Kuntz, I. D. (1979) *Biopolymers 18*, 73.

Havel, T. F., Kuntz, I. D., & Crippen, G. M. (1983) *Bull. Math. Biol. 45*, 665.

Heilmann, J., Barollier, J., & Watzke, E. (1957) *Hoppe-Seyler's Z. Physiol. Chem. 309*, 219.

Hirs, C. H. W. (1967) *Methods Enzymol. 11*, 197.

Hosur, R. V., Wider, G., & Wüthrich, K. (1983) *Eur. J. Biochem. 130*, 497.

James, T. L., Young, G. B., Broido, M. S., Keepers, J. W., Jamin, N., & Zon, G. (1985) *J. Biosci. 8*, 553.

Kassell, B. (1970) *Methods Enzymol. 19*, 844.

Kumar, A., Wagner, G., Ernst, R. R., & Wüthrich, K. (1980) *Biochem. Biophys. Res. Commun. 96*, 1156.

Lowry, O. H., Rosebrough, N. J., Farr, A. L., & Randell, R. J. (1951) *J. Biol. Chem. 193*, 265.
March, S. C., Parikh, I., & Cuatrecasas, P. (1974) *Anal. Biochem. 60*, 149.
McCammon, J. A., & Karplus, M. (1983) *Acc. Chem. Res. 16*, 187.
Moonen, C. T. W., Scheek, R. M., Boelens, R., & Müller, F. (1984) *Eur. J. Biochem. 141*, 323.
Pardi, A., Wagner, G., & Wüthrich, K. (1983) *Eur. J. Biochem. 137*, 445.
Pearson, G. A. (1977) *J. Magn. Reson. 27*, 265.
Reisfeld, R. A., Lewis, U. J., & Williams, D. E. (1962) *Nature (London) 195*, 281.
Rousselet, A., Faure, G., Boulain, J.-C., & Ménez, A. (1984) *Eur. J. Biochem. 140*, 31.
Schmidt, P. G., & Kuntz, I. D. (1984) *Biochemistry 23*, 4261.
Solomon, I., & Bloembergen, N. (1956) *J. Chem. Phys. 25*, 261.
Stassinopoulou, C. I., Wagner, G., & Wüthrich, K. (1984) *Eur. J. Biochem. 145*, 423.
Vincent, J.-P., & Lazdunski, M. (1973) *Eur. J. Biochem. 38*, 365.
Wagner, G., & Wüthrich, K. (1982a) *J. Mol. Biol. 155*, 347.
Wagner, G., & Wüthrich, K. (1982b) *J. Mol. Biol. 160*, 343.
Weiss, M. A., Eliason, J. L., & States, D. J. (1984) *Proc. Natl. Acad. Sci. U.S.A. 81*, 6019.
Wien, R. W., Morrisett, J. D., & McConnell, H. M. (1972) *Biochemistry 11*, 3707.
Williamson, M. P., Marion, D., & Wüthrich, K. (1984) *J. Mol. Biol. 173*, 341.
Williamson, M. P., Havel, T. F., & Wüthrich, K. (1985) *J. Mol. Biol. 182*, 295.
Wüthrich, K., Wider, G., Wagner, G., & Braun, W. (1982) *J. Mol. Biol. 155*, 311.
Yamada, S., & Itano, H. A. (1966) *Biochim. Biophys. Acta 130*, 538.

Proton NMR Studies of Plastocyanin: Assignment of Aromatic and Methyl Group Resonances from Two-Dimensional Spectra†

Garry C. King‡ and Peter E. Wright*
Department of Inorganic Chemistry, University of Sydney, Sydney, NSW 2006, Australia
Received November 14, 1985

ABSTRACT: Two-dimensional NMR methods have been used to assign aromatic and methyl group resonances in the ^{1}H NMR spectra of French bean and poplar plastocyanins. Specific assignments are presented for all 11 of the aromatic spin systems and 32 methyl group resonances of French bean plastocyanin. A further nine methyl group resonances are attributed to individual spin systems but have not yet been specifically assigned. For poplar plastocyanin, 10 aromatic spin systems and 20 methyl group resonances are specifically assigned. Assignments to specific amino acids are based on the X-ray structure of poplar plastocyanin. The assignment problem has been simplified by using the two-dimensional spectra of oxidized plastocyanin as subspectra of protons distant from the copper center. Two-dimensional relayed coherence transfer spectra were particularly useful for making unambiguous assignments of Ala, Thr, and aromatic spin systems. A discrepancy between the NMR spectra and amino acid sequence of poplar Pc at residue 39 is observed.

Plastocyanin (Pc)[1] is a blue copper protein (M_r 10600) that functions as an essential component of the photosynthetic electron transport chain (Boulter et al., 1977). Many types of physicochemical studies have been performed on Pc, placing it among the best characterized of the electron transfer proteins. High-resolution crystal structures have been determined for both oxidation states of poplar plastocyanin under a variety of crystallization conditions (Colman et al., 1978; Freeman, 1981; Guss & Freeman, 1983). A structure of the apoprotein, which differs very little from that of the holoprotein, has also been reported (Garrett et al., 1984). This wealth of crystallographic information on Pc has not been matched by detailed data on its solution conformation and dynamics, which are potentially obtainable from ^{1}H NMR experiments. High-resolution ^{1}H NMR has been previously applied to Pc for an investigation of the electron self-exchange reaction (Beattie et al., 1975), identification of resonances from groups near the copper center (Markley et al., 1975; Ulrich & Markley, 1978; Hill & Smith, 1978; Kojiro & Markley, 1983), an examination of structural conservation between species by overall spectral comparison (Freeman et al., 1978a,b), and location of protein binding sites for inorganic electron transfer reagents (Cookson et al., 1980a,b; Handford et al., 1980). These earlier studies have produced only a few specific resonance assignments; most were carried out in the absence of a crystal structure and before recent improvements in NMR methodology became commonly available. Remarkably, as

† This work was supported by the Australian Research Grants Scheme (Grant D2 82/15284). G.C.K. acknowledges the receipt of a Commonwealth Postgraduate Research Award.
* Address correspondence to this author at the Department of Molecular Biology, Research Institute of Scripps Clinic, La Jolla, CA 92037.
‡ Present address: Department of Molecular Biophysics and Biochemistry, Yale University, New Haven, CT 06510.

[1] Abbreviations: Pc, plastocyanin; 2D, two-dimensional; 2D*J*, two-dimensional *J*-resolved spectroscopy; COSY, two-dimensional scalar correlated spectroscopy; RCT, two-dimensional relayed coherence transfer spectroscopy; NOESY, two-dimensional dipolar correlated spectroscopy; NOE, nuclear Overhauser effect; FID, free induction decay; pt, point.

0006-2960/86/0425-2364$01.50/0